Contents lists available at ScienceDirect

Food Chemistry: Molecular Sciences

Comparison of oxidative stress-mitochondria-mediated tenderization in two different bovine muscles during aging

Zhenjiang Ding [a,b,1], Qichao Wei [a,1], Chunmei Liu [a], Chunhui Zhang [a], Feng Huang [a,*]

[a] Institute of Food Science and Technology, Chinese Academy of Agricultural Sciences/Key Laboratory of Agro-Products Processing, Ministry of Agriculture and Rural Affairs, Beijing 100193, China
[b] Beijing Key Laboratory of the Innovative Development of Functional Staple and Nutritional Intervention for Chronic Diseases, China National Research Institute of Food and Fermentation Industries, Beijing 100015, China

ABSTRACT

The aim of this study was to investigate the differences in the effects of mitochondria-involved energy metabolism and caspases activation on postmortem tenderness in different muscle fiber types. Beef *Longissimus thoracis* (LT) and *Psoas major* (PM) muscles showed significant difference in mitochondrial function. Our data revealed that PM suffered from higher levels of reactive oxygen species (ROS) earlier than LT, causing faster mitochondrial swelling and rupture. Additionally, faster metabolism of ATP-related compounds and activation of caspase-9 appeared in PM, but the activity of caspase-3 in PM was lower than that in LT. Differences in myofibril fragmentation index (MFI) of LT and PM at different aging stages suggested that energy metabolism and caspases activities may play a role in tenderness at different aging stages. These results indicated that oxidative stress-mitochondria-mediated tenderization process could be muscle-specific.

1. Introduction

Tenderness is a key term used to describe meat quality and consumers would pay a premium to purchase guaranteed-tender meat. The conversion of muscle to meat was a complex biochemical process and the meat quality after slaughter was characterized by morphological and biochemical properties of muscles (Kim, Yang, & Jeong, 2018). With the loss of function of the organism system postmortem, the antioxidant system in muscle cells can not resist the massive accumulation of reactive oxygen species (ROS), inducing oxidative stress (Lana & Zolla, 2015). Whereas, the role of ROS in proteolysis and meat tenderization remains unclear. Changes in the structure of myofibrillar proteins caused by oxidative modifications, making them more susceptible to enzymatic degradation (Ding, Wei, Zhang, Zhang, & Huang, 2021). On the contrary, ROS promoted toughness by inhibiting the activity of µ-calpain that mediated myofibrillar proteins degradation (Ouali et al., 2006).

Mitochondria are the main site of ROS generation and principal target of oxidation. The regulation mechanism of mitochondria on postmortem tenderization may involve two aspect. On one hand, ROS disrupted membrane permeability transition pore (MPTP) and promoted

mitochondrial anion fluxes (Lana & Zolla, 2015), inducing water to be forced to enter into mitochondria. The constant water caused mitochondria to swell and even rupture (Kaasik, Safiulina, Zharkovsky, & Veksler, 2007). The increase in mitochondrial permeability triggered the release of cytochrome *c* from the mitochondria to the cytoplasm, resulting in the activation of caspase-9, which in turn initiated the caspase-3 cascade (Ding et al., 2021). Effector caspases performed the apoptotic step by cleaving cytoskeletal proteins including vimentin, desmin and spectrin (Wang, 2000), and then played a key role in the tenderization of postmortem meat. On the other hand, mitochondrial dysfunction promoted glycolytic flux and ATP hydrolysis, inducing pH decline and regulation of postmortem tenderization (Matarneh et al., 2017). Analogously, inhibitors of mitochondria complexes altered the content of glycolytic intermediate metabolite and ATP-related compounds (Scheffler, Matarneh, England, & Gerrard, 2015). ATP generated by glycolysis was hydrolyzed to produce H^+ ions, which further triggered the drop in pH, rather than caused by the accumulation of lactate (Yu, Tian, Shao, Li, & Dai, 2020). ATP was an essential molecule for the actomyosin complex, and the content of ATP-related compounds affected the movement of actin and myosin, regulating sarcomere contraction and relaxation (Lana & Zolla, 2015). Thus, the

* Corresponding author at: No. 1, Nongda South Rd., Xi Beiwang, Haidian District, Beijing 100193, China.
  E-mail address: fhuang226@163.com (F. Huang).
[1] Both authors contributed equally to the work.

mitochondrial pathway may play an important role in postmortem meat tenderization.

The skeletal muscles of different parts of the animal body were composed of heterogeneous muscle fibers and had different inherent physiological functions, such as metabolism and contractile response (Picard & Gagaoua, 2020). Through myosin ATPase staining and histochemical techniques, the muscle fiber types of Chinese simmental cattle can be divided into type I, type IIA and type IIB, with different cross-sectional area and glycolytic rates (Lang et al., 2020). *Psoas major* (PM) muscle fibers, which were mainly composed of type I (slow-oxidative fibers, red fibers), has a higher percentage of myoglobin and mitochondrial content than *longissimus dorsi* (LD) muscle fibers, which were mainly composed of type IIX (fast-glycolytic fibers, white fibers) (Jeong et al., 2009; Picard & Gagaoua, 2020). Additionally, oxidative and glycolytic fibers utilized oxidative phosphorylation and glycolysis to generate ATP, respectively (Picard, Ritchie, Thomas, Wright, & Hepple, 2011). The LD, PM and *semimembranosus* (SM) of cattle were used to explore the relationship between muscle fiber characteristics and meat quality traits, the difference in the composition of muscle fiber types resulted in differences in ultimate pH, moisture content, and sarcomere length, which in turn led to differences in tenderness (Hwang, Kim, Jeong, Hur, & Joo, 2010). Different muscle fiber types had different mitochondrial content, which influenced glycolytic rates and myofibrillar protein degradation, and ultimately affected meat quality (Picard & Gagaoua, 2020). Besides, several studies have revealed significant differences in collagen content, calpain/calpastatin ratios (Ouali & Talmant, 1990), and the degree of myofibrillar proteins degradation (desmin and troponin T) (Muroya, Ertbjerg, Pomponio, & Christensen, 2010) among different muscle fiber types. Previous studies suggested that most of differentially abundant proteins and metabolites between *longissimus lumborum* (LL) and PM involved multiple pathways occurred in mitochondria through proteomics and metabolomics (Yu et al., 2018, 2020). Thus, it could be hypothesized that mitochondria occupied a noteworthy position in tenderness differences involved in muscle fiber-specificity among different skeletal muscles during postmortem. The objective of this study was to compare the differences in ROS-mitochondrial pathway-mediated tenderization in two beef skeletal muscles postmortem (*Longissimus thoracis* and *Psoas major*). It was hoped that the data can improve the postmortem tenderization mechanism of different muscle fiber types.

2. Materials and methods

2.1. Animals and muscle sampling

Six simmental cattle (average live weight 450 kg) were Halal slaughtered (GB/T 17237–2008) at a commercial meat processing company (Beijing Zhuochen Animal Husbandry Co., Ltd., Beijing, China) according to the Animal Care and Ethics Committee of Chinese Academy of Agricultural Sciences (IAS20160616, Beijing, China). All cattle were raised on the same farm with the same diet and then slaughtered on the same day. In this study, the *Longissimus thoracis* (LT) and PM muscles were removed from the carcasses within 30 min. Each muscle (LT and PM) was further separated into six equal-size sections per carcass for six aging period, and 36 slices were obtained from six cattle (six replications per muscle and per aging period). The samples were individually vacuum-packaged in a polyolefin bag and randomly assigned to aging at 4 °C. The muscles were obtained at 0, 6, 12, 24, 72 and 120 h postmortem and immediately frozen in liquid nitrogen after pH measurement and samples preparation of electron microscope.

2.2. Detection of ROS

The level of ROS was determined according to the method described by Zhang, Li, Yu, Han, and Ma (2019). Approximately 1 g samples were homogenized in four volumes of precooled buffer containing 10 mmol/L

Tris, 0.1 mmol/L ethylenediaminetetraacetic acid disodium salt (EDTA-2Na), 10 mmol/L sucrose, and 0.8 % NaCl, pH 7.4, and then centrifuged at 3,000 g and 4 °C for 15 min. Subsequently, the obtained supernatant was incubated with the buffer (1:1 vol/vol) containing 2′,7′-dichlorohydrofluorescein diacetate (DCFH-DA, 10 μM) at 37 °C for 0.5 h. The fluorescence was measured in a fluorometer equipped (SynergyH1M, BioTek, USA) at 480/525 nm (excitation wavelength/emission wavelength).

2.3. Isolation of mitochondria and measurement of mitochondrial membrane potential

The mitochondrial protein was extracted following the method reported by Wang et al. (2018) with slight modifications. The minced muscle was homogenized in the precooled buffer (1:10 wt/vol) containing 2 mmol/L EDTA, 70 mmol/L sucrose, 5.0 mmol/L 4-morpholine-propanesulphonic acid (MOPS), 220 mmol/L mannitol and 0.5 % bovine serum albumin (BSA), pH 7.4. The supernatant after centrifugation at 1500 g and 4 °C for 10 min was centrifuged again at 12,000 g and 4 °C for 20 min. Subsequently, the pellet was resuspended in suspension buffer (extraction buffer without BSA), and the suspension was centrifuged at 12,000 g and 4 °C for 10 min. The final pellet was resuspended in suspension buffer to obtain the mitochondrial-enriched protein fraction. The protein concentration was determined with a BCA protein assay kit and adjusted to the same. The mitochondrial membrane potential (MMP) was detected by JC-1 assay kit (CA1310-100, Solarbio, China). 0.1 mL mitochondrial protein (1 mg/mL) was incubated with JC-1 staining working solution (1:9 vol/vol) for 20 min. The fluorescence intensity was detected by a fluorescence spectrophotometer (SynergyH1M, BioTek, USA). The wavelengths were 490/530 nm (excitation wavelength/emission wavelength) and 525/590 nm (excitation wavelength/emission wavelength), respectively. The red/green fluorescence intensity ratio was used to indicate the level of MMP.

2.4. Transmission electron microscope observation

Strips (1 mm × 1 mm × 5 mm) were cut from two muscles (LT and PM) at each storage time point for transmission electron microscopy (TEM). The samples were fixed with 2.5 % glutaraldehyde in 0.1 mol/L phosphate buffer, and fixed again with 2 % osmium tetroxide. After being dehydrated by the gradually increasing concentrations of ethanol solutions, the samples were dehydrated with acetone, followed being infiltrated with propylene oxide and embedded with resin. Ultrathin sections were cut using a ultra-microtome (PowerTome-XL, RMC, USA) and stained with uranyl acetate and lead citrate. The mitochondrial images were captured using a transmission electron microscope (H-7500, Hitachi, Japan) (Feng et al., 2020; Yu et al., 2020).

2.5. Detection of caspase-3 and caspase-9 activity

Caspase-3 assay kit (K533, Biovision, USA) and caspase-9 assay kit (K118, Biovision, USA) were used to detect caspase-3 activity and caspase-9 activity, respectively. The samples were homogenized with cold lysis buffer for three 10 s bursts at a speed of 15000 rpm, and the homogenate was centrifuged at 15,000 g and 4 °C for 15 min to obtained sarcoplasmic proteins. The protein concentration was detected with a BCA protein assay kit and adjusted to 5 mg/mL. The sarcoplasmic proteins were mixed with equal volume of 2 × reaction buffer (contain DTT), and then 5 μL of the LEHD-AFC (caspase-9 substrate) and Ac-DEVD-AFC (caspase-3 substrate) were added for caspase-9 and caspase-3 activity, respectively. The fluorescence was measured in a fluorometer equipped (SynergyH1M, BioTek, USA) at 400/505 nm (excitation wavelength/emission wavelength) after the mixture was incubated at 37 °C for 2 h (Ding et al., 2021).

2.6. Detection of ATP-related compounds

The ATP-related compounds were extracted and detected using the procedure of Fan, Chi, and Zhang (2008) with slight modifications. The minced muscle (approximately 1 g) was homogenized in of 10 % perchloric acid solution (1:2 wt/vol), and centrifuged at 1500 g and 4 °C for 10 min. The pellet was washed with 2 mL of 5 % perchloric acid solution and centrifuged under the same conditions. The pH value of supernatants was adjusted to 6.4 using NaOH. Perchloric acid solution (pH 6.4) was used to replenish the volume of the supernatants to 10 mL after centrifugation.

The supernatants were filtered through a 0.2 mm membrane filter and analysed for ATP-related compounds using HPLC (1260 Infinity II, Agilent, USA) equipped with Diode array detector (DAD) and Inertsil ODS-35 μm column (4.6 × 250 mm). The sample was injected at a flow rate of 1 mL/min, and the mobile phase was 0.05 mol/L phosphate buffer solution (pH 6.8). The identification of the peak was accomplished by comparing its retention times and spectral characteristics with the standard substances (ATP, ADP, AMP and IMP).

2.7. Detection of pH

The samples were homogenized in a buffer (1:8 wt/vol) containing 5 mmol/L iodoacetic acid and 150 mmol/L KCl (pH 7.0). The meat homogenates were centrifuged at 10,000 g for 5 min, and equilibrated to 25 °C. The pH meter (FiveEasy Plus, Mettler Toledo, USA) was calibrated at room temperature using pH 4.01, 6.86 and 9.18 standard buffer before the pH measurement.

2.8. Detection of myofibril fragmentation index

The myofibril fragmentation index (MFI) was detected using the procedure of Wang et al. (2019) with slight modifications. The minced muscle (approximately 0.5 g) was homogenized in ice-cold buffer (1:10 wt/vol) containing 100 mmol/L KCl, 1 mmol/L MgCl$_2$, 20 mmol/L K$_2$HPO$_4$ and 1 mmol/L EDTA, pH 7.0. The samples were centrifuged at 3000 g and 4 °C for 15 min. The obtained precipitate was resuspended in aforementioned buffer and centrifuged under the same conditions. The precipitate was next resuspended in the buffer and filtered through a nylon sieve (20 mesh). The protein concentration of the filtrate was detected by the biuret method, and then the concentration was adjusted to 0.5 mg/mL. The absorbance at 540 nm was detected and the result was multiplied by 200 to obtain the MFI value.

2.9. Statistical analyses

The data were expressed as means ± SD from 3 to 6 replicates using the SPSS statistical software package (IBM, Chicago, IL, USA). LSD and Duncan's multiple range test ($p < 0.05$) was used to compare the differences in different times during postmortem aging from the same skeletal muscle. Student's *t* test was used to compare the differences in different skeletal muscles at the same time during postmortem aging.

3. Results and discussion

3.1. ROS content

The generation of ROS including hydrogen peroxide, superoxide anions and hydroxyl radicals in cells and tissues was inevitable (Yu et al., 2020). DCFH-DA can be deacetylated by esterases in cells because of its good permeability to generate DCFH (non-fluorescent), then reacted with ROS and transformed into high DCF. Consequently, the ROS content in the two muscles was examined by staining with DCFH-DA. As shown in Fig. 1, the ROS content of LT decreased from 0 h to 12 h ($p < 0.05$), and increased from 12 h to 120 h during postmortem aging ($p < 0.05$). The ROS content of PM decreased from 0 h to 6 h ($p < 0.05$), and
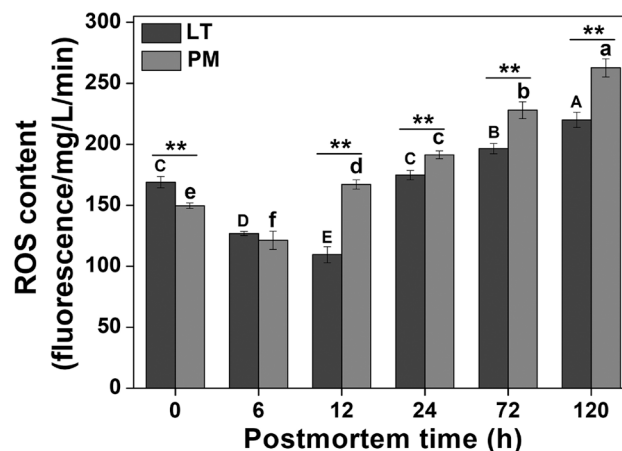
Fig. 1. The changes of ROS content in LT and PM muscles during postmortem aging. Data are presented as mean ± SD. Different letters (a–f) are significant difference ($p < 0.05$). Different letters (A–E) are significant difference ($p < 0.05$). ** $p < 0.01$.

increased from 6 h to 120 h during postmortem aging ($p < 0.05$). Additionally, the ROS content of PM was higher than that of LT from 12 h to 120 h during postmortem aging, respectively ($p < 0.01$). Analogously, ROS levels in the muscles showed a trend of decline first, then rise during postmortem aging, and the minimum appeared at 6 h or 12 h (Zhang et al., 2019). Interestingly, Yu et al. (2020) testified that ROS levels of PM was significantly higher than that of LL at 24 h postmortem, but there was no significant difference in the ROS level at 6 h. There were many antioxidant systems including glutathione system and thioredoxin system maintained the balance between the elimination and generation of cellular ROS. The decrease in the ROS content during the early postmortem period could result from the antioxidant systems partially clearing the ROS (Wedgwood, Dettman, & Black, 2001). Once the lack of blood flow led to failure of adaptive mechanisms of cells to maintain homeostasis, the antioxidant systems were destroyed, inducing oxidative stress (Ke et al., 2017).

3.2. MMP and mitochondrial morphology

ROS was mainly produced by mitochondria and regulated by one or more complexes of the mitochondrial respiratory chain (Lana & Zolla, 2015; Wang et al., 2018). Inversely, oxidative stress would result in increased mitochondrial membrane permeability and mitochondrial fission (Wang et al., 2018). MMP reflected the mitochondria membrane permeability, that was, the degree of openness of mitochondrial membrane pores. Normal MMP was very important for mitochondria to perform the necessary physiological functions (Zhang, Ma, & Kim, 2020). The JC-1 was used to measure the MMP indicated that the lower the red/green fluorescence ratio was, the lower the MMP, representing the greater mitochondrial membrane permeability. As shown in Fig. 2 A, LT had a sustained decrease in MMP throughout the whole postmortem aging ($p < 0.05$). The MMP of PM was at a low level, and there was a significant decrease at 0–72 h postmortem ($p < 0.05$), but no changes were obtained at 72–120 h postmortem ($p > 0.05$). Comparing the MMP of the two muscles at the same time, it could be found that the MMP of LT was higher than that of PM at 0–72 h postmortem ($p < 0.05$). Additionally, the MMP of LT at 24 h postmortem and PM at 12 h postmortem was basically the same. LT had the same MMP at 72 h postmortem as PM at 24 h postmortem. The TEM was performed to further examine the influence of muscle fiber types on the mitochondrial morphological changes in the postmortem ageing of meat (Fig. 2 B). The mitochondrial morphology of the two muscles was condensed, and the cristae was evenly distributed at 0 h. The mitochondrial morphology of LT and PM showed swelling (typical matrix vacuolation) at 24 h and 12
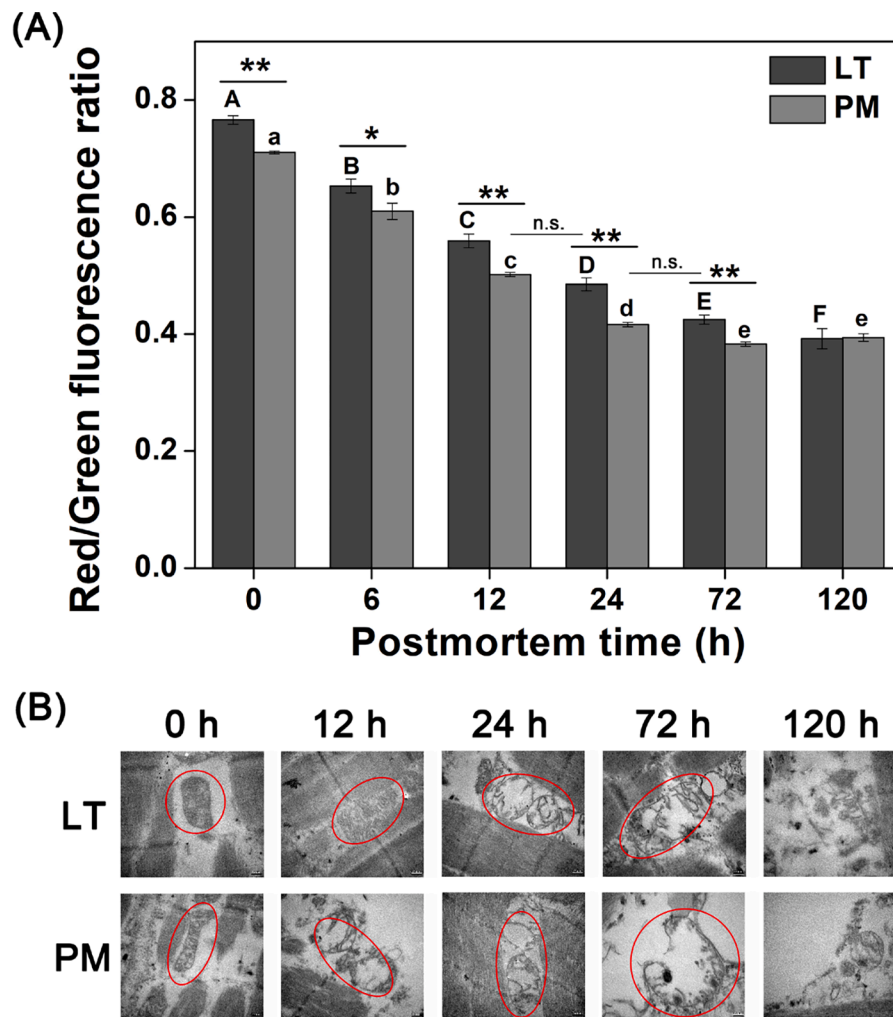
Fig. 2. The changes of MMP (A) and mitochondrial morphology (B) in LT and PM muscles during postmortem aging. Scale bar = 0.2 μm. Data are presented as mean ± SD. Different letters (a–e) are significant difference ($p < 0.05$). Different letters (A–F) are significant difference ($p < 0.05$). * $p < 0.05$, ** $p < 0.01$.

h postmortem, respectively. The mitochondria of LT and PM showed severe cristae degradation and dissolution of the outer membrane at 120 h and 72 h postmortem, respectively. Overall, the MMP and mitochondrial morphology in the present study illuminated that mitochondrial dysfunction occurred at different time in different muscle fiber types. Disruption of mitochondrial function in PM preceded LT and may be associated with more severe oxidative stress. Similarly, Zhang et al. (2020) compared the mitochondrial membrane permeability of LD and PM of pork muscles during postmortem aging, and found that the mitochondrial membrane permeability of LD was lower than that of PM, and the mitochondrial membrane permeability of LD continued to increase throughout the whole postmortem aging, while the mitochondrial membrane permeability of PM only increased significantly in the early stage. The MMP of LL and PM muscles from cattle decreased remarkably during postmortem aging, and LL showed significantly higher MMP than PM at 24 h postmortem (Yu et al., 2020). Ke et al. (2017) also demonstrated that the level of mitochondrial degradation was greater in PM than LL by examining the changes in mitochondrial content. Simultaneously, the cristae content of the mitochondria of beef LT at 24 and 72 h postmortem was greatly decreased, the matrix was more transparent, and the inner membrane was discontinuous and degraded (Li et al., 2020).

3.3. Caspase-3 and caspase-9 activities

With the disruption of mitochondrial cristae and MPTP, cytochrome

c released from mitochondrial cristae and bound apoptotic protease activating factor-1 (Apaf-1) to form apoptosomes, resulting in apoptosis (Ding et al., 2021). Similarly, Thornberry and Lazebnik (1998) reported that caspase-9-mediated intrinsic pathway was involved in the caspase-3 activation. The degradation of myofibrillar proteins involved in caspase-3 could reflect the effect of conditioning on meat tenderness (Kemp, Parr, Bardsley, & Buttery, 2006). Herein, the activities of caspase-9 and caspase-3 in LT and PM were assessed as shown in Fig. 3. The caspase-9 activities in LT and PM both increased first and then decreased, and reached the maximum at 12 h and 6 h after slaughter, respectively. Similarly, caspase-3 activity in LT and PM both increased significantly from 0 h to 24 h and peaked at 24 h. The results clarified that the time of caspase-9 reached the highest activity was earlier than that of caspase-3, which consistent with the previous studies (Wang et al., 2018; Zhang et al., 2019). The caspase-9 activity in PM reached its peak earlier than LT, which may be closely related to the earlier occurrence of mitochondrial dysfunction in PM and the trend of ROS changes. Moreover, the results of the differences in the caspase-3 and caspase-9 activities in LT and PM were basically consistent with the results of caspases activities in different parts of in bovine skeletal muscles detected by Cao et al. (2013), and the results of caspase-3 activities in LD and PM of pigs (Zhang et al., 2020). The inconsistent results of caspase-9 and caspase-3 activities in different parts of skeletal muscles may be associated the multiple pathways including death receptor pathway, endoplasmic reticulum pathway, and mitochondrial pathway, which could activate caspase-3.
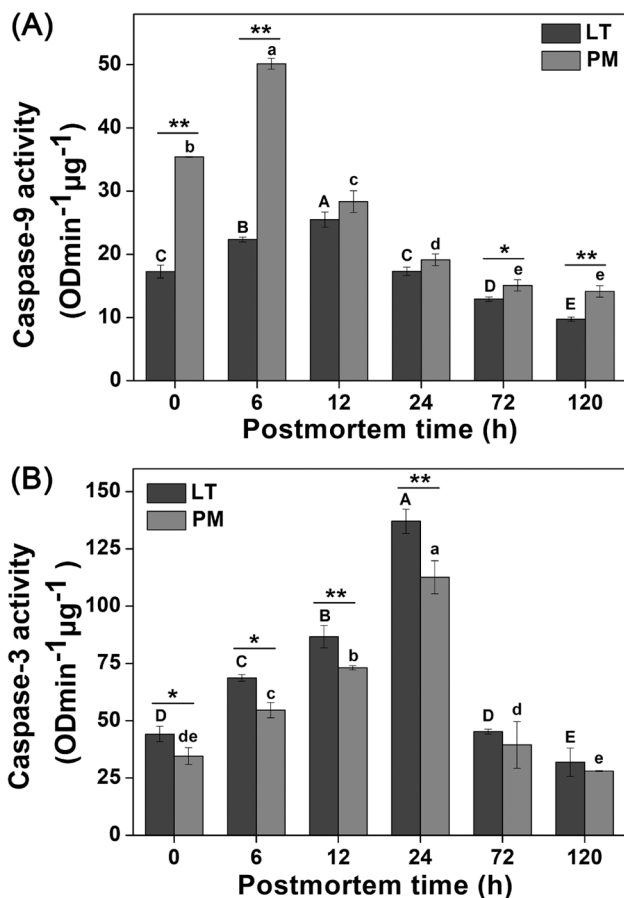
Fig. 3. The changes of caspase-9 activity (A) and caspase-3 activity (B) in LT and PM muscles during postmortem aging. Data are presented as mean ± SD. Different letters (a–e) are significant difference ($p < 0.05$). Different letters (A–E) are significant difference ($p < 0.05$). * $p < 0.05$, ** $p < 0.01$.

3.4. ATP-related compounds content

Intracellular ATP was degraded rapidly due to the rapid consumption of glycogen and insufficient oxygen supply during postmortem ischemia (Du, Shen, & Zhu, 2005). Intriguingly, ATP was recognized to activate caspase-9 (Delivoria-Papadopoulos, Gorn, Ashraf, & Mishra, 2007), and intracellular ATP content was one of the factors that determined whether cells undergone apoptosis or necrosis (Fujimura, Morita-Fujimura, Murakami, Kawase, & Chan, 1998). The intracellular ATP-related compounds content in LT and PM were determined (Fig. 4). The initial content and decline rate of ATP in PM were higher than those in LT (Fig. 4A). Similarly, the depletion of ATP was faster in the PM than in the LD, and the ultimate ATP concentration appeared at 24 h and 12 h in LD and PM of bulls, respectively (Kim, Kim, Lee, & Baik, 2000). Liu, Kim, Yang, Jemmerson, and Wang (1996) revealed that the depletion of ATP prevented the activation of caspase-9. Hence, ATP may directly or indirectly regulate the activity of caspase-9, and was one of the reasons why the activity of caspase-9 in PM was higher than that in LT. Additionally, the change trend of ADP in LT and PM is basically the same as that of ATP (Fig. 4B). The AMP content in LT and PM both increased first and then decreased, and reached the maximum at 72 h after slaughter. Compared with LT, AMP content in PM was higher at 6–120 h postmortem ($p < 0.05$) (Fig. 4C). The change trend of IMP in LT and PM is basically the same as that of AMP except for peak time (Fig. 4D). The mitochondrial ATPase may play a role in hydrolysis of ATP, rather than ATP production postmortem. Mitochondrial proteins content and mitochondrial function may vary by biological types, affecting energy levels (Hudson, 2012). Once consumption of ATP was greater than

production under non-steady state conditions, adenylate kinase or myokinase produced additional ATP through the reaction: $ADP + ADP \rightarrow ATP + AMP$. Conversion from AMP to IMP was mediated by AMP deaminase: $AMP + H^+ \rightarrow IMP + NH_4^+$. The above two reactions occurred when the bioenergetic function of mitochondria was reduced and could not meet the ATP required by the cells (Ferguson & Gerrard, 2014). Muroya, Oe, Nakajima, Ojima, and Chikuni (2014) also revealed that IMP reached maximum content at 24 h postmortem in the LL, and the peak time of AMP content in vastus intermedius was earlier than that in LL may be caused by the higher activity of adenylate kinase. Consequently, ATP was degraded at different rates between LT and PM on the pathway $ATP \rightarrow ADP \rightarrow AMP \rightarrow IMP$. The difference in the content of ATP-related compounds in LT and PM may be due to the higher mitochondria density of type I, including enzymatic systems that allow oxygen consumption and the electron transport chain, to provide energy by increasing oxygen consumption, while type IIX was mainly through glycolytic metabolism (Picard & Gagaoua, 2020).

3.5. pH

As we mentioned earlier, mitochondrial regulation of postmortem tenderization can be divided into two aspects (regulation of energy metabolism and pH; release of apoptotic factors). In fact, there is also a cross-talk between the two aspects. Energy level and pH were the main factors affecting apoptosis and internal environment during postmortem aging (Chen et al., 2020). Changes in pH affected the release of mitochondrial apoptotic factors and the activation of apoptotic enzymes (Matsuyama, Llopis, Deveraux, Tsien, & Reed, 2000). Compared with LT, PM showed lower pH values especially at 0 h postmortem ($p < 0.05$). Additionally, pH decreased during postmortem aging and finally reached ultimate values at 24 h in the LT or PM (Fig. 5). The difference in pH may be related to the difference in ATP hydrolysis efficiency caused by different fiber compositions of LT and PM (Yu et al., 2018). PM possesses high content of type I fibers resulting in a predominant oxidative metabolism, whereas type IIA fibers were found in LL and consequently exhibited more glycolytic metabolism (Hwang et al., 2010).

3.6. MFI

Measurement of MFI was a useful method to determine I band rupture and proteolysis postmortem (Feng et al., 2020). The MFI of LT and PM was observed as shown in Fig. 6. LT and PM had an increase in MFI throughout the whole postmortem aging, indicating a progressive increase in breakage of interstitial fibril connection and degradation of key structural proteins. Besides, the MFI of PM at 6 h and 12 h postmortem was significantly higher than that of LT, which may be due to the significantly higher rate of change of energy metabolism (ATP-related compounds) in PM than in LT at early postmortem period. Changes in the content of ATP-related compounds not only affected the transshipment capacity of ADP/ATP translocase 1, regulating the Warner-Bratzler Shear Force (WBSF) of postmortem meat (Li et al., 2019). It also regulated the phosphorylation level of proteins, which in turn affects pH and the activities of endogenous enzymes (Wang et al., 2019). Intriguingly, the relative activity of μ-calpain was higher in PM muscles than that in LL result from the more suitable pH (Wang et al., 2019). Additionally, the actomyosin complex was able to dissociate only in the presence of ATP, the mechanical movement of myosin pushed back the linked actin filament, resulting in the shortening of sarcomeres and contraction (Lana & Zolla, 2015). Nevertheless, the MFI of PM at 72 h and 120 h postmortem was lower than that of LT ($p < 0.01$). Marino, Della Malva, and Albenzio (2015) revealed that higher MFI was found in LD than PM muscle at late postmortem period. This was consistent with the result that the activity of caspase-3 in PM was lower than that in LT. Our previous research showed that caspase-3 promoted the degradation of titin, nebulin and troponin-T (Ding et al., 2018). Accordingly, we
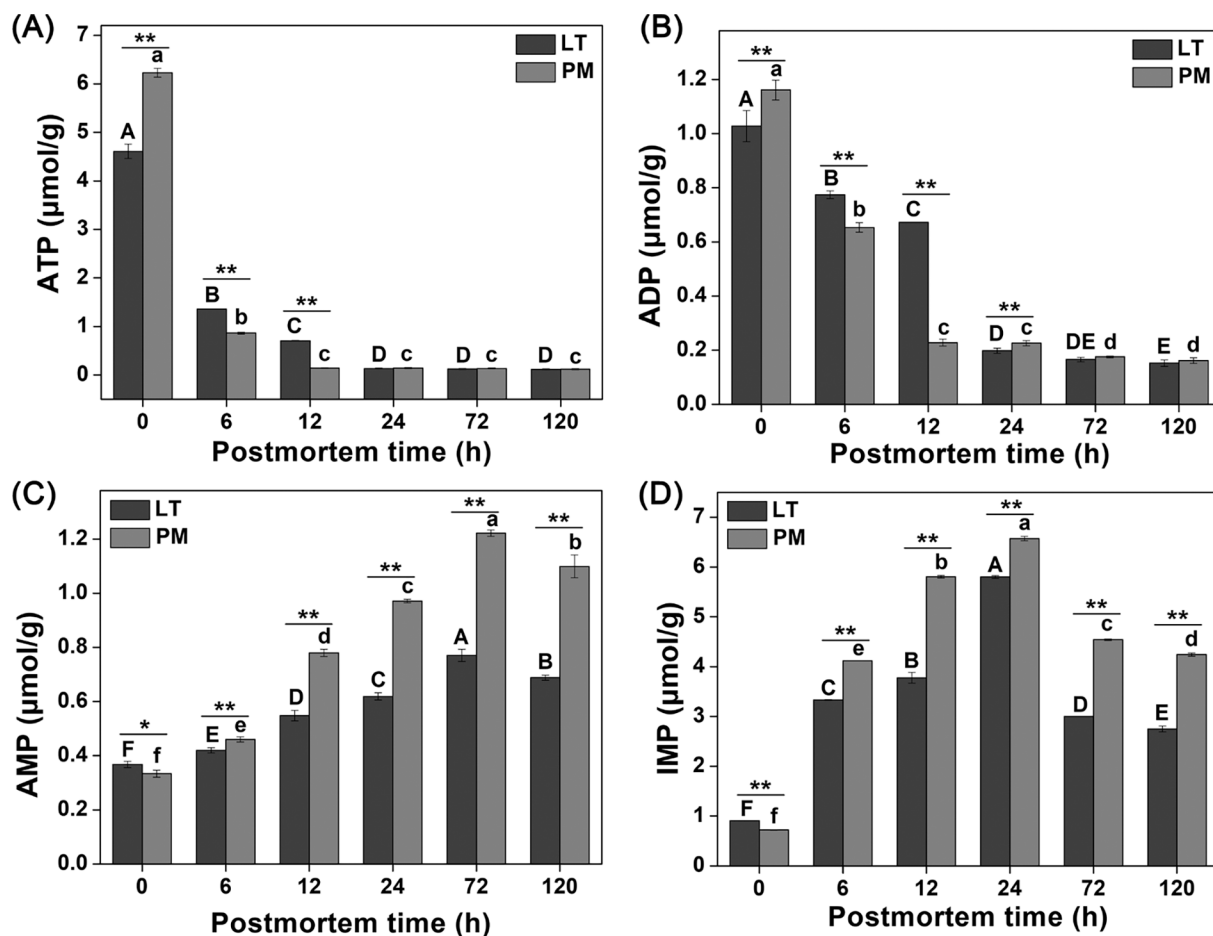
Fig. 4. The changes of ATP (A), ADP (B), AMP (C) and IMP (D) in LT and PM muscles during postmortem aging. Data are presented as mean $\pm$ SD. Different letters (a–f) are significant difference ($p < 0.05$). Different letters (A–F) are significant difference ($p < 0.05$). * $p < 0.05$, ** $p < 0.01$.
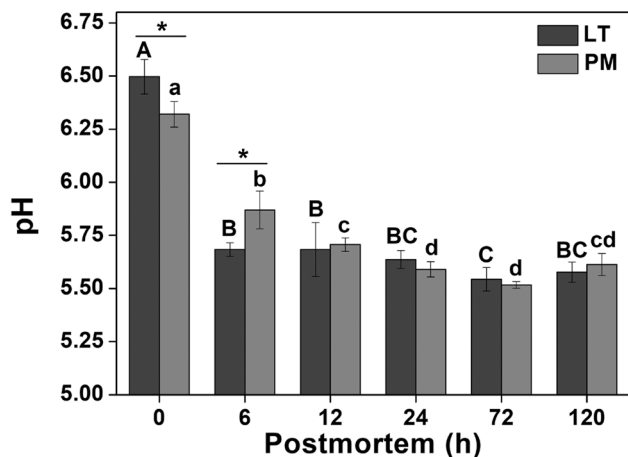
Fig. 5. The changes of pH in LT and PM muscles during postmortem aging. Data are presented as mean $\pm$ SD. Different letters (a–d) are significant difference ($p < 0.05$). Different letters (A–C) are significant difference ($p < 0.05$). * $p < 0.05$.

Fig. 6. The changes of MFI in LT and PM muscles during postmortem aging. Data are presented as mean $\pm$ SD. Different letters (a–d) are significant difference ($p < 0.05$). Different letters (A–F) are significant difference ($p < 0.05$). ** $p < 0.01$.

speculated that the differences in myofibrillar protein fragmentation and degradation in LT and PM may be related to the role of energy metabolism and caspases activities at different postmortem stages.

At physiological conditions, the oxygen consumption of mitochondria was really strong to meet the normal metabolism of muscle cells, and the intermediate metabolites that reduced O_2 to H_2O were ROS,

such as $O_2^{\cdot-}$, H_2O_2 and $^{\cdot}OH$ (Lana & Zolla, 2015). The intracellular antioxidant barriers (superoxide dismutase, catalase, peroxidase, thioredoxin system and glutathione system, etc.) maintained ROS levels below an appropriate threshold level so that there was no risk of ROS toxicity. With the loss of metabolic function and weakened antioxidant

system in muscle cells postmortem, the level of ROS in muscle cells increased dramatically, causing oxidative stress (Ke et al., 2017). Mitochondria were not only the main source of ROS, but also the main target of ROS. Mitochondria could affect postmortem tenderization by regulating energy metabolism and releasing apoptotic factors, and there was also a cross-talk between the two aspects. It was well established that muscles were composed of different percentages of fibers. Oxidative and glycolytic fibers differed in both ATP and ROS metabolism in muscle cells (Picard et al., 2011). Therefore, the comparison of ROS-mitochondrial mediated postmortem tenderization in different muscle fiber types became the focus of our research. Our results showed that ROS levels in LT and PM showed a trend of decline first, then rise during postmortem aging, and the minimum appeared at 12 h and 6 h, respectively. This may be related to the role of antioxidant systems in muscle cells at early postmortem period. The MMP of PM was significantly lower than that of LT during postmortem aging, and mitochondrial swelling and rupture occurred preferentially, which was consistent with the comparison of mitochondrial membrane permeability in LD and PM of pork muscles during postmortem aging (Zhang et al., 2020). Overall, muscles composed of different muscle fiber types had different timings of ROS-mediated mitochondrial dysfunction during postmortem aging. The mitochondrial pathway was one of the key pathways for inducing apoptosis. In the present study, the time points of caspase-9 activity reached the maximum value in both LT and PM were earlier than that of caspase-3. The results were similar to Zhang et al. (2019) which observed that activation of caspase-9 occurred before the activation of caspase-3. Notably, the results of caspase-3 and caspase-9 activities in LT and PM were consistent with the results in bovine skeletal muscles detected by Cao et al. (2013). Besides, mitochondria could regulate glycolytic flux and ATP hydrolysis, which in turn affected postmortem tenderness (Matarneh et al., 2017). Interestingly, the metabolic rate of ATP-related compounds in PM was higher than that in LT. This may be the reason why the MFI of PM was higher than that of LT at early postmortem period.

4. Conclusion

Oxidative stress-mediated mitochondrial function differed in muscles composed of different muscle fiber types. PM exhibited a rapid onset of oxidative stress and mitochondrial dysfunction compared to LD, evidenced by ROS level, MMP, mitochondrial morphology, caspase-9 activity and content of ATP-related compounds. The difference of MFI in LT and PM may be related to the role of energy metabolism and caspases activities at different postmortem stages. This novel mechanism further provided support for understanding the effects of different muscle fiber types on postmortem tenderization.

Declaration of Competing Interest

The authors declare that they have no known competing financial interests or personal relationships that could have appeared to influence the work reported in this paper.

Acknowledgment

References

Cao, J. X., Ou, C. R., Zou, Y. F., Ye, K. P., Zhang, Q. Q., Khan, M., … Zhou, G. (2013). Activation of caspase-3 and its correlation with shear force in bovine skeletal muscles during postmortem conditioning. *Journal of Animal Science, 91*(9), 4547–4552.

Chen, C., Zhang, J., Guo, Z., Shi, X., Zhang, Y., Zhang, L., … Han, L. (2020). Effect of oxidative stress on AIF-mediated apoptosis and bovine muscle tenderness during postmortem aging. *Journal of Food Science, 85*(1), 77–85.

Delivoria-Papadopoulos, M., Gorn, M., Ashraf, Q. M., & Mishra, O. P. (2007). ATP and cytochrome c-dependent activation of caspase-9 during hypoxia in the cerebral cortex of newborn piglets. *Neuroscience letters, 429*(2–3), 115–119.

Ding, Z., Huang, F., Zhang, C., Zhang, L., Sun, H., & Zhang, H. (2018). Effect of heat shock protein 27 on the *in vitro* degradation of myofibrils by caspase-3 and μ-calpain. *International Journal of Food Science and Technology, 53*(1), 121–128.

Ding, Z., Wei, Q., Zhang, C., Zhang, H., & Huang, F. (2021). Influence of oxidation on Heat Shock Protein 27 translocation, caspase-3 and calpain activities and myofibrils degradation in postmortem beef muscles. *Food Chemistry, 340*, Article 127914.

Du, M., Shen, Q. W., & Zhu, M. J. (2005). Role of β-adrenoceptor signaling and AMP-activated protein kinase in glycolysis of postmortem skeletal muscle. *Journal of Agricultural and Food Chemistry, 53*(8), 3235–3239.

Fan, W., Chi, Y., & Zhang, S. (2008). The use of a tea polyphenol dip to extend the shelf life of silver carp (Hypophthalmicthys molitrix) during storage in ice. *Food Chemistry, 108*(1), 148–153.

Feng, Y. H., Zhang, S. S., Sun, B. Z., Xie, P., Wen, K. X., & Xu, C. C. (2020). Changes in physical meat traits, protein solubility, and the microstructure of different beef muscles during post-mortem aging. *Foods, 9*(6), 806.

Ferguson, D., & Gerrard, D. (2014). Regulation of post-mortem glycolysis in ruminant muscle. *Animal Production Science, 54*(4), 464–481.

Fujimura, M., Morita-Fujimura, Y., Murakami, K., Kawase, M., & Chan, P. H. (1998). Cytosolic redistribution of cytochrome c after transient focal cerebral ischemia in rats. *Journal of Cerebral Blood Flow & Metabolism, 18*(11), 1239–1247.

Hudson, N. J. (2012). Mitochondrial treason: A driver of pH decline rate in post-mortem muscle? *Animal Production Science, 52*(12), 1107–1110.

Hwang, Y. H., Kim, G. D., Jeong, J. Y., Hur, S. J., & Joo, S. T. (2010). The relationship between muscle fiber characteristics and meat quality traits of highly marbled Hanwoo (Korean native cattle) steers. *Meat Science, 86*(2), 456–461.

Jeong, J. Y., Hur, S. J., Yang, H. S., Moon, S. H., Hwang, Y. H., Park, G. B., & Joo, S. T. (2009). Discoloration characteristics of 3 major muscles from cattle during cold storage. *Journal of Food Science, 74*(1), C1–C5.

Kaasik, A., Safiulina, D., Zharkovsky, A., & Veksler, V. (2007). Regulation of mitochondrial matrix volume. *American Journal of Physiology-Cell Physiology, 292*(1), C157–C163.

Ke, Y., Mitacek, R. M., Abraham, A., Mafi, G. G., VanOverbeke, D. L., DeSilva, U., & Ramanathan, R. (2017). Effect of muscle-specific oxidative stress on cytochrome c release and oxidation-reduction potential properties. *Journal of Agriculture and Food Chemistry, 65*(35).

Kemp, C., Parr, T., Bardsley, R., & Buttery, P. (2006). Comparison of the relative expression of caspase isoforms in different porcine skeletal muscles. *Meat Science, 73*(3), 426–431.

Kim, K., Kim, Y., Lee, Y., & Baik, M. (2000). Postmortem muscle glycolysis and meat quality characteristics of intact male Korean native (Hanwoo) cattle. *Meat Science, 55*(1), 47–52.

Kim, G. D., Yang, H. S., & Jeong, J. Y. (2018). Intramuscular variations of proteome and muscle fiber type distribution in semimembranosus and semitendinosus muscles associated with pork quality. *Food Chemistry, 244*, 143–152.

Lana, A., & Zolla, L. (2015). Apoptosis or autophagy, that is the question: Two ways for muscle sacrifice towards meat. *Trends in Food Science & Technology, 46*(2), 231–241.

Lang, Y., Zhang, S., Xie, P., Yang, X., Sun, B., & Yang, H. (2020). Muscle fiber characteristics and postmortem quality of longissimus thoracis, psoas major and semitendinosus from Chinese Simmental bulls. *Food Science & Nutrition, 8*(11), 6083–6094.

Li, S., Yu, Q., Han, L., Zhang, Y., Tian, X., & Zhao, S. (2019). Effects of proteome changes on the tenderness of yak rumen smooth muscle during postmortem storage based on the label-free mass spectrometry. *Food Research International, 123*, 1336–1343.

Li, X., Zhang, D., Ijaz, M., Tian, G., Chen, J., & Du, M. (2020). Colour characteristics of beef longissimus thoracis during early 72 h postmortem. *Meat Science, 170*, Article 108245.

Liu, X., Kim, C. N., Yang, J., Jemmerson, R., & Wang, X. (1996). Induction of apoptotic program in cell-free extracts: Requirement for dATP and cytochrome c. *Cell, 86*(1), 147–157.

Marino, R., Della Malva, A., & Albenzio, M. (2015). Proteolytic changes of myofibrillar proteins in Podolian meat during aging: Focusing on tenderness. *Journal of Animal Science, 93*(3), 1376–1387.

Matarneh, S. K., England, E. M., Scheffler, T. L., Yen, C. N., Wicks, J. C., Shi, H., & Gerrard, D. E. (2017). A mitochondrial protein increases glycolytic flux. *Meat Science, 133*, 119–125.

Matsuyama, S., Llopis, J., Deveraux, Q. L., Tsien, R. Y., & Reed, J. C. (2000). Changes in intramitochondrial and cytosolic pH: Early events that modulate caspase activation during apoptosis. *Nature Cell Biology, 2*(6), 318–325.

Muroya, S., Ertbjerg, P., Pomponio, L., & Christensen, M. (2010). Desmin and troponin T are degraded faster in type IIb muscle fibers than in type I fibers during postmortem aging of porcine muscle. *Meat Science, 86*(3), 764–769.

Muroya, S., Oe, M., Nakajima, I., Ojima, K., & Chikuni, K. (2014). CE-TOF MS-based metabolomic profiling revealed characteristic metabolic pathways in postmortem porcine fast and slow type muscles. *Meat Science, 98*(4), 726–734.

Ouali, A., Herrera-Mendez, C. H., Coulis, G., Becila, S., Boudjellal, A., Aubry, L., & Sentandreu, M. A. (2006). Revisiting the conversion of muscle into meat and the underlying mechanisms. *Meat Science, 74*(1), 44–58.

Ouali, A., & Talmant, A. (1990). Calpains and calpastatin distribution in bovine, porcine and ovine skeletal muscles. *Meat Science, 28*(4), 331–348.

Picard, B., & Gagaoua, M. (2020). Muscle fiber properties in cattle and their relationships with meat qualities: An overview. *Journal of Agricultural and Food Chemistry, 68*(22), 6021–6039.

Picard, M., Ritchie, D., Thomas, M. M., Wright, K. J., & Hepple, R. T. (2011). Alterations in intrinsic mitochondrial function with aging are fiber type-specific and do not explain differential atrophy between muscles. *Aging cell, 10*(6), 1047–1055.

Scheffler, T. L., Matarneh, S. K., England, E. M., & Gerrard, D. E. (2015). Mitochondria influence postmortem metabolism and pH in an in vitro model. *Meat Science, 110,* 118–125.

Thornberry, N. A., & Lazebnik, Y. (1998). Caspases: Enemies within. *Science, 281*(5381), 1312–1316.

Wang, K. K. (2000). Calpain and caspase: Can you tell the difference? *Trends in Neurosciences, 23*(1), 20–26.

Wang, Y., Li, X., Li, Z., Du, M. T., Zhu, J., Zhang, S. Q., & Zhang, D. Q. (2019). Phosphorylation of sarcoplasmic and myofibrillar proteins in three ovine muscles during postmortem ageing. *Journal of Integrative Agriculture, 18*(7), 1643–1651.

Wang, L. L., Yu, Q. L., Han, L., Ma, X. L., Song, R.-D., Zhao, S. N., & Zhang, W. H. (2018). Study on the effect of reactive oxygen species-mediated oxidative stress on the activation of mitochondrial apoptosis and the tenderness of yak meat. *Food Chemistry, 244*, 394–402.

Wedgwood, S., Dettman, R. W., & Black, S. M. (2001). ET-1 stimulates pulmonary arterial smooth muscle cell proliferation via induction of reactive oxygen species. *American Journal of Physiology-Lung Cellular and Molecular Physiology, 281*(5), L1058–L1067.

Yu, Q., Tian, X., Shao, L., Li, X., & Dai, R. (2020). Mitochondria changes and metabolome differences of bovine longissimus lumborum and psoas major during 24 h postmortem. *Meat Science, 166*, Article 108112.

Yu, Q., Tian, X., Shao, L., Xu, L., Dai, R., & Li, X. (2018). Label-free proteomic strategy to compare the proteome differences between longissimus lumborum and psoas major muscles during early postmortem periods. *Food Chemistry, 269*, 427–435.

Zhang, J., Li, M., Yu, Q., Han, L., & Ma, Z. (2019). Effects of lysosomal–mitochondrial apoptotic pathway on tenderness in post-mortem bovine longissimus muscle. *Journal of Agricultural and Food Chemistry, 67*(16), 4578–4587.

Zhang, J., Ma, D., & Kim, Y. H. B. (2020). Mitochondrial apoptosis and proteolytic changes of myofibrillar proteins in two different pork muscles during aging. *Food Chemistry, 319*, Article 126571.